Journal of
Synchrotron
Radiation

ISSN 1600-5775

Received 28 June 2013
Accepted 30 September 2013

A low-cost X-ray-transparent experimental cell for synchrotron-based X-ray microtomography studies under geological reservoir conditions

Florian Fusseis,[a]* Holger Steeb,[b] Xianghui Xiao,[c] Wen-lu Zhu,[d] Ian B. Butler,[a] Stephen Elphick[a] and Urs Mäder[e]

[a]School of Geosciences, The University of Edinburgh, Grant Institute, King's Buildings, West Mains Road, Edinburgh EH9 3JW, UK, [b]Institute of Mechanics, Ruhr-University Bochum, Universitätsstrasse 150, Bochum 44801, Germany, [c]Beamline 2BM, 431-B002, Advanced Photon Source, Argonne National Laboratory, 9700 South Cass Avenue, Argonne, IL 60439, USA, [d]Department of Geology, University of Maryland, College Park, MD 20742, USA, and [e]Institute of Geological Sciences, University of Bern, Baltzerstrasse 1+3, Bern 3012, Switzerland. *E-mail: florian.fusseis@ed.ac.uk

A new modular X-ray-transparent experimental cell enables tomographic investigations of fluid rock interaction under natural reservoir conditions (confining pressure up to 20 MPa, pore fluid pressure up to 15 MPa, temperature ranging from 296 to 473 K). The portable cell can be used at synchrotron radiation sources that deliver a minimum X-ray flux density of 10^9 photons mm^{-2} s^{-1} in the energy range 30–100 keV to acquire tomographic datasets in less than 60 s. It has been successfully used in three experiments at the bending-magnet beamline 2BM at the Advanced Photon Source. The cell can be easily machined and assembled from off-the-shelf components at relatively low costs, and its modular design allows it to be adapted to a wide range of experiments and lower-energy X-ray sources.

Keywords: high-energy microtomography; *in situ* studies; porous media.

1. Introduction

Movement of fluids in rock is of fundamental interest for geothermal energy and fossil fuel extraction, CO_2 sequestration and nuclear waste storage. Fluids interacting with rocks critically affect the rocks' mechanical and chemical properties at all scales, from crystal lattice to plate tectonic (*e.g.* Griggs, 1967; Regenauer-Lieb *et al.*, 2001). Consequently, the behaviour and migration of fluids in rocks have been extensively studied [see reviews by, for example, Rumble (1989), Ferry (1994) and Ingebritsen & Manning (2010) for metamorphic fluid migration]. Laboratory studies used to rely on indirect measurements and *post mortem* analyses to quantify the various aspects of fluid migration in porous rocks [see, for example, Kranz *et al.* (1990) and David *et al.* (1994) amongst numerous others], but over the last 25 years techniques such as magnetic resonance imaging, neutron and X-ray tomography have changed our experimental approaches [see, for example, Kimmich (1997), Kaestner *et al.* (2008), Webber (2012) and Wildenschild & Sheppard (2013) for overviews]. However, only the latest generation of synchrotron-based X-ray microtomography beamlines are capable of imaging fluid flow and fluid–rock interactions in cells that are robust enough to simulate conditions in geological reservoirs. Here we present a simple and cost-effective experimental cell that allows imaging of fluid–rock interaction at confining pressures of up to 20 MPa and temperatures up to 473 K. So far, the cell has been successfully employed in three experiments at beamline 2-BM at the Advanced Photon Source (USA).

2. The experimental cell and its periphery

The cell is a miniature version of a Hassler core holder with independent control of confining pressure and fluid infiltration. It consists of upper and lower stainless steel end-caps that hold an X-ray-transparent aluminium pressure vessel containing the millimetre-sized sample in between them (Figs. 1 and 2). Three support rods with threaded ends connect to nuts at the upper and lower end-caps and support the confining pressure applied in the cell. All connections for the confining oil and pore fluid circuits are through high-pressure liquid chromatography fittings in the upper and lower end-caps of the cell. The fittings connect to short stainless steel tubes, which themselves connect to flexible PEEK (polyether ether ketone) tubes to allow the cell to rotate freely on the rotation stage. A small spill container is attached to the base of the cell, which itself connects to a magnetic base that fits the air-bearing stages available at the beamline. The cell uses commercially available components where possible and readily available materials for parts that need to be machined (Fig. 2). Parts, materials and suppliers are listed in Table S1 of the supporting information, as well as technical drawings of the machined parts.[1]

The sample is mounted inside the central aluminium pressure vessel, in between two stainless steel tube stubs. The lower stub is permanently threaded into the base, whereas the upper stub is

[1] Supporting information for this paper is available from the IUCr electronic archives (Reference: PP5039).

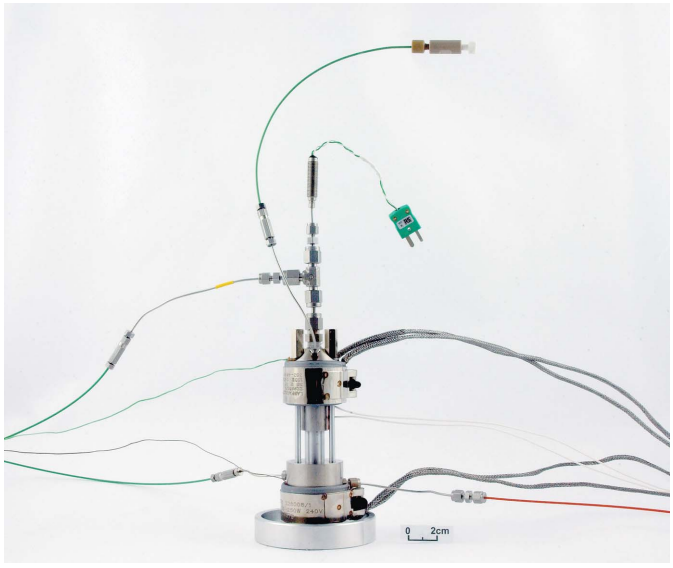

Figure 1
The assembled cell, with the two bracket heaters mounted around the upper and lower end-caps and the internal thermocouple inserted through the top of the cell. Note that, in experimental use, a magnetic base is fixed to the bottom spill container, which connects to the air-bearing stage at the beamline. See text for further explanation.

inserted through the top, is adjusted to the sample height and held in place using a fitting on the upper end-cap. Currently, the cell can accommodate cylindrical samples with diameters of up to 3 mm. The length of the sample is defined by the application and field of view. The sample is jacketed by a combination of elastic silicone and high-temperature heat shrink tubes and sealed from the confining silicone oil through a combination of O-rings and windings of thin steel wire that provided an excellent seal (see Fig. S1).

In our experiments, confining pressure is applied to the sample using a manually operated piston screw pump (Fig. 2). The heat-resistant confining oil is pumped into the space between the wall of the aluminium pressure vessel and the jacketed sample. Confining pressure is monitored using a pressure gauge at the pump. An adjustable pressure-release valve prevents overpressurization. Multiple-day experiments were conducted at a confining pressure of 15 MPa, with a higher pressure reached over short periods and during the off-line safety testing. The central pressure vessel has a wall thickness of 4 mm, is made from cold-worked aluminium, and is specified to withstand a bursting pressure of up to 60 MPa. We also tested a pressure vessel and support rods made from 6082-T6 alloy and found that these components are fully compatible with the beamline set-up. 6082-T6 aluminium alloy has a proof stress of 310 MPa, resulting in a bursting strength of the aluminium vessel of 172 MPa. Due to the substantially increased safety margin, we recommend using this alloy to machine the pressure vessel and support rods (see also Table S1).

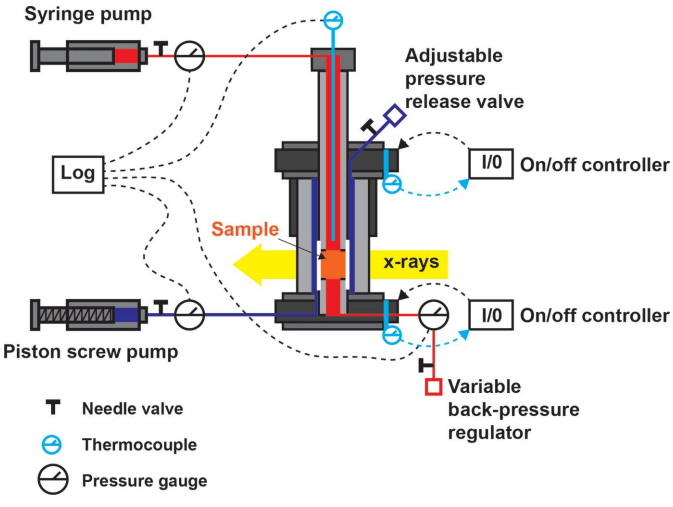

Figure 2
Sketch of the set-up of the cell and its peripheral hardware.

Fluid can be pumped through the sample using a high-pressure syringe pump (Fig. 2). At the down-stream end an adjustable back-pressure regulator sets the pore fluid pressure. Fluid pressure is monitored using pressure gauges before and after the sample.

The cell is heated by two band heaters mounted around the upper and lower end-caps (Figs. 1 and S2), with a supporting heating mat wrapped around the upper half of the aluminium pressure vessel to counter excessive thermal loss. The heaters are monitored by two adhesive type-K thermocouples mounted in between the heaters and the cell and controlled by two on–off controllers (Table S1). A third, sheathed, thermocouple is inserted into the fluid pressure circuit through the top of the cell, with the tip placed a few millimetres above the sample, sealed and held in place by a fitting at the top of the cell. This thermocouple is logged remotely. The temperature difference between the heaters and the sample was found to be 15 K (at 473 K heater temperature). A thermal insulation shield sandwiched in between the spill container and the magnetic base minimizes conductive heat loss towards the rotating stage.

The modularity of the cell allows for individual parts to be exchanged and adapted to specific experimental requirements. Besides the heated cell shown in Fig. 1, a second ambient-temperature, low confining/pore fluid pressure (up to 373 K, up to 5 MPa) cell uses fibre-glass reinforced PEEK (Table S1) for the top and base parts and quartz glass cylinders for the central X-ray-transparent part (see supporting technical drawings). This cell is used for fluid infiltration/imbibition experiments at ambient temperature and under low pore- and confining pressure conditions ($\leq$1 MPa).

3. Data acquisition and application

The cell was tested and improved at beamline 2-BM at the Advanced Photon Source. Beamline 2-BM is a dedicated tomography beamline with a bending-magnet source. Experiments were conducted in the upstream experimental station 25 m from the source. There, a polychromatic beam filtered by 1 mm aluminium, 15 mm silicon and 8 mm borosilicate glass yielded a photon flux with an energy peak at 65 keV (Fig. S3). The filters were used to eliminate X-rays below 30 keV, which would have introduced beam-hardening artefacts. A Cooke pco.dimax CMOS camera with 2016 $\times$ 2016 pixels (pixel size 11 µm $\times$ 11 µm) was used in a scan mode in which projections are recorded while the sample is continuously rotated (*i.e.* the stage rotation does not stop in between image acquisitions). The camera recorded projections from a 100 µm-thick LuAG:Ce single-crystal scintillator, magnified through a 7.5$\times$ Mitutoyo long-working-distance lens yielding a pixel side length of 1.47 µm. The sample–scintillator distance was 300 mm. Projections were collected with an exposure time of 10 ms while the sample was rotated over 180° at 9° s^{-1}. 1800 projections were collected in 20 s. A single-distance phase retrieval algorithm (Paganin *et al.*, 2002) was used to reconstruct tomographic datasets.

So far the heated (i) and ambient-temperature (ii, iii) cells have been successfully used in three experiments (Fig. S4), all of which are still being analysed:

(i) Real-time evolution of pore structure during *in situ* carbonation of porous olivine aggregates (forsterite, Mg_2SiO_4). In an olivine carbonation experiment a sintered olivine sample was subjected to a constant confining pressure P_c of 15 MPa while a sodium bicarbonate solution ($NaHCO_3$ at 1.5 *M*) was injected into the olivine sample at a fluid pressure of 10 MPa. Subsequently, the cell was heated to 473 K for a total duration of $\sim$72 h. Under these conditions, olivine dissolution and magnesite ($MgCO_3$) precipitation cause considerable alteration in the existing pore space. Microtomography datasets collected at different stages of the carbonation process reveal progressive growth of new crystals [Fig. S4(*a*)].

(ii) Oil/water imbibition experiments in a dolomitic reservoir rock to reproduce results from Pak *et al.* (2013) with a higher temporal resolution than achieved with a laboratory tomograph in Edinburgh. A KI-doped aqueous solution was replaced with dodecane [$CH_3(CH_2)_{10}CH_3$], a low viscosity alkane [Fig. S4(*b*)]. This experiment was conducted at ambient temperature and under a moderate confining pressure P_c of 1 MPa [Fig. S4(*b*)].

(iii) Infiltration of dodecane [$CH_3(CH_2)_{10}CH_3$] and KI-doped aqueous solution into a reservoir sandstone across the top surface of the sample to study boundary effects. This experiment was conducted at ambient temperature and under a moderate confining pressure P_c of 1 MPa.

4. Conclusions

We present a simple experimental cell that allows microtomographic visualization of fluid flow and fluid–rock interaction in porous rocks at reservoir conditions. The cell is designed for synchrotron-based X-ray microtomography and so far has been used at the bending-magnet source beamline 2-BM at the Advanced Photon Source. Successful tests proved that it allows for fast (*i.e.* in seconds) scanning of a millimetre-sized sample at 473 K and 15 MPa using a polychromatic beam with a photon flux larger than 10^9 photons mm^{-2} s^{-1} in the energy range between 30 and 100 keV. Its simplicity and modularity allow for the design to be adapted to specific experimental requirements and lower-energy sources easily and make the cell a low-cost platform for future technical developments. The cell contributes towards investigating a wide range of geological reservoirs in time-resolved three-dimensional studies. The time- and space-resolved experiments that become possible with the cell will contribute significantly to our understanding of the dynamics of geothermal reservoirs, CO_2 sequestration and high-level radioactive waste repositories.

Use of the Advanced Photon Source at Argonne National Laboratory was supported by the US Department of Energy (DOE), Office of Science, Office of Basic Energy Sciences, under Contract No. DE-AC02-06CH11357. The olivine carbonation study was partially funded by DOE under grant DOE#C11E10947 (WZ). We thank Harrison Lisabeth for his participation in the olivine carbonation experiments at 2-BM. Tannaz Pak is thanked for preparation of and valuable advice during experiment (ii). Technical support by Thomas Siegenthaler, Stefan Seifert, Petra Nagel, Lothar Kühne, Bob Brown and Alex Hard is gratefully acknowledged.

References

David, C., Wong, T.-F., Zhu, W. & Zhang, J. (1994). *Pure Appl. Geophys.* **143**, 425–456.
Ferry, J. M. (1994). *J. Geophys. Res.* **99**, 15487–15498.
Griggs, D. (1967). *Geophys. J. Int.* **14**, 19–31.
Ingebritsen, S. E. & Manning, C. E. (2010). *Geofluids*, **10**, 193–205.
Kaestner, A., Lehmann, E. & Stampanoni, M. (2008). *Adv. Water Resour.* **31**, 1174–1187.
Kimmich, R. (1997). *NMR: Tomography, Diffusometry, Relaxometry*. Berlin: Springer.
Kranz, R. L., Saltzman, J. S. & Blacic, J. D. (1990). *Int. J. Rock Mech. Min. Sci.* **27**, 345–352.
Paganin, D., Mayo, S. C., Gureyev, T. E., Miller, P. R. & Wilkins, S. W. (2002). *J. Microsc.* **206**, 33–40.
Pak, T., Butler, I. B., van Dijke, R., Geiger, S. & Jiang, Z. (2013). *1st International Conference on Tomography of Materials and Structures*, Ghent, Belgium, 1–5 July 2013.
Regenauer-Lieb, K., Yuen, D. A. & Branlund, J. (2001). *Science*, **294**, 578–580.
Rumble, D. (1989). *Eur. J. Mineral.* **1**, 731–737.
Webber, B. (2012). *Physics*, **5**, 14.
Wildenschild, D. & Sheppard, A. P. (2013). *Adv. Water Resour.* **51**, 217–246.